

Preliminary performance evaluation of a high resolution small animal PET scanner with monolithic crystals and depth-of-interaction encoding

Marcin Balcerzyk, George Kontaxakis, *Senior Member, IEEE*, Mercedes Delgado, Luis Garcia, Jose M. Benlloch, Miguel A. Pozo

Abstract— A preliminary user evaluation of the Albira small animal PET scanner is presented. The system has $\text{Ø}80 \times 40 \text{ mm}^2$ field of view. In the center of the field of view it has 0.8% sensitivity with 33% solid angle coverage. Maximum of noise equivalent counts is 25kcps for 8.9 MBq for a mouse phantom. The scanner employs an innovative crystal design of only eight $40(50) \times 40(50) \times 9.8$ mm LYSO tapered monolithic crystals forming detector modules read by position sensitive photomultipliers. This design allows easy depth of interaction readout. The system saturates at 8.9 MBq for the mouse phantom. As an example of application of the Albira system, some preliminary results from a study on animal models on ischemic stroke with 18-FDG co-registered with MRI images are shown.

I. INTRODUCTION

SMALL animal positron emission tomography (PET) scanners are becoming now a widespread tool for pre-clinical research. In this study we present the new Albira (Oncovision, Valencia, Spain) small animal PET scanner from the user point of view.

II. GENERAL SCANNER CHARACTERISTICS

A. System description

The dimensions of the Albira PET scanner, shown in Fig. 1, are $75 \times 75 \times 60 \text{ cm}^3$. Its field of view (FOV) has dimensions $\text{Ø}80 \times 40 \text{ mm}^3$. The moving bed can hold a rat or a mouse. The anesthesia system can be mounted via the FOV opening. Once a month, the system requires calibration. This is performed with $35 \times 35 \times 1 \text{ mm}^3$ phantom filled with 18-FDG. Daily the detectors are being tested by a special program before starting experiments. Data are acquired in list mode.

Manuscript received August 18, 2008. This work was supported in part by the Comunidad de Madrid grant MULTIMAG. M. Balcerzyk was supported by Marie-Curie fellowship MEIF-CT-2006-041482

Marcin Balcerzyk is with the Instituto Pluridisciplinar, Universidad Complutense de Madrid, Madrid 28040, Spain (corresponding author, tel: +34 91 394 3261; fax: +34 91 394 3266; e-mail: m.balcerzyk@pluri.ucm.es).

Mercedes Delgado, Luis Garcia and Miguel A. Pozo are with Instituto Pluridisciplinar, Univ. Complutense de Madrid, Madrid, 28040, Spain

George Kontaxakis is with ETSI Telecomunicación, Univ. Politécnica de Madrid, and with Networking Research Center on Bioengineering, Biomaterials and Nanomedicine (CIBER-BBN), Madrid, Spain.

José M. Benlloch is with Instituto de Física Corpuscular, Universidad de Valencia and CSIC, Valencia, Spain

The system offers three basic configurable modes of operation:

- static study without any bed movement;
- dynamic study with variable time duration for each frame, delay between frames and bed movement in three dimensions within the FOV;
- so called “bed study”, where whole body of the animal is studied with movement of the bed. Typical mouse study requires three bed positions, while a rat study requires four.

The system includes two computers running Windows XP (Microsoft Corp., Redmont, WA). One of them is used for data acquisition and storing, and the other for image reconstruction and processing tasks. The system is connected through local area network with 1.3 TB RAID 5 disk storage system.



Fig. 1 Photo of the small animal PET system.

The scanner employs an innovative crystal design of only eight $40(50) \times 40(50) \times 9.8 \text{ mm}^3$ LYSO tapered crystals forming detector modules read by position sensitive photomultipliers. The detectors have 18% singles efficiency (55% stopping power, about 50% photo-fraction and 33% solid angle coverage). Detectors use Hamamatsu H8500 $49 \times 49 \text{ mm}^2$ position sensitive photomultipliers. Standard coincidence window is 5 ns, reconfigurable to 3, 5, 8 or 11

ns. The energy resolution for 511 keV is 14%. The design of large continuous tapered crystal detectors allows easy depth of interaction readout, but results in saturation of the system at 8.9 MBq for mouse phantom.

B. Acquisition modes and data management

The basic logical unit for the management of a system is a “Study”. It can contain several acquisitions performed in modes specified above. A Study has a Subject – an animal of specified weight, and date of birth. Studies are carried out by a specified User. Parameters of the Study can be stored in a Study Protocol. An interface to Acquirer module is shown in Fig. 2.



Fig. 2 The Acquirer interface.

There is Manager module to handle an increasing number of Studies and Subjects and prepare Protocols of data acquisition and image reconstruction. It allows searching for specific Study, Subject, User, etc., preparing a new Study ahead of time, and retrieving it just before the Acquisition. The Manager interface is shown in Fig. 3.

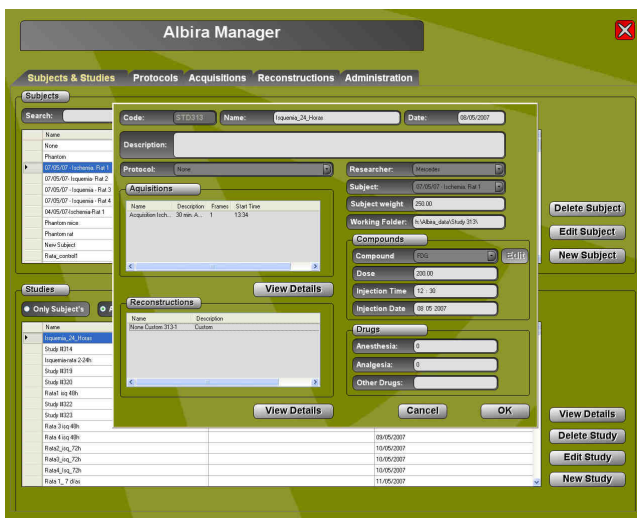


Fig. 3 Manager interface.

C. Image Reconstruction

There are two modes of iterative image reconstruction: MLEM (Maximum Likelihood Expectation Maximization) and OSEM (Ordered Subset Expectation Maximization). MLEM typically iterates 12 cycles, while OSEM iterates for 3 cycles over all subsets. These algorithms can be combined with correction for radioisotope decay, scatter and randoms. The image reconstruction parameters combined with the mode of the Study can be stored in the Reconstruction Protocol. There is a possibility of reconstruction of individual files specifying all parameters manually. List mode data can be regrouped to form new time frame(s), or a static study file can be divided into several frames, if that is necessary after Acquisition.

Image reconstruction can be performed in smaller ($40 \times 40 \times 40 \text{ mm}^3$) and larger ($\varnothing 80 \times 40 \text{ mm}^3$) FOV with $0.5 \times 0.5 \times 0.5 \text{ mm}^3$ voxel size. Typical reconstruction time in smaller FOV is 5 min per frame and 30 min per frame in larger FOV. For the studies with a specified image reconstruction Protocol, batch mode reconstruction can be applied for overnight reconstructions. The Reconstructor interface is shown in Fig. 4.



Fig. 4 Reconstructor interface.

D. Image analysis

The images can be viewed and manipulated by bundled commercial research software PMOD [1]. The platform allows visualization, image fusion with other modalities, model kinetic analysis, pixel-wise modeling and 3D rendering at a very advanced level. In our lab, a typical PET study is preceded by a magnetic resonance study (MRI, T2 weighted, $128 \times 128 \times 128$ pixels, 0.3125 mm pixel size) to reveal anatomical details and allow coregistration with the PET images.

We have developed a model system for its simulation using the GATE platform [2]. The tool yields list mode files ready for image reconstruction.

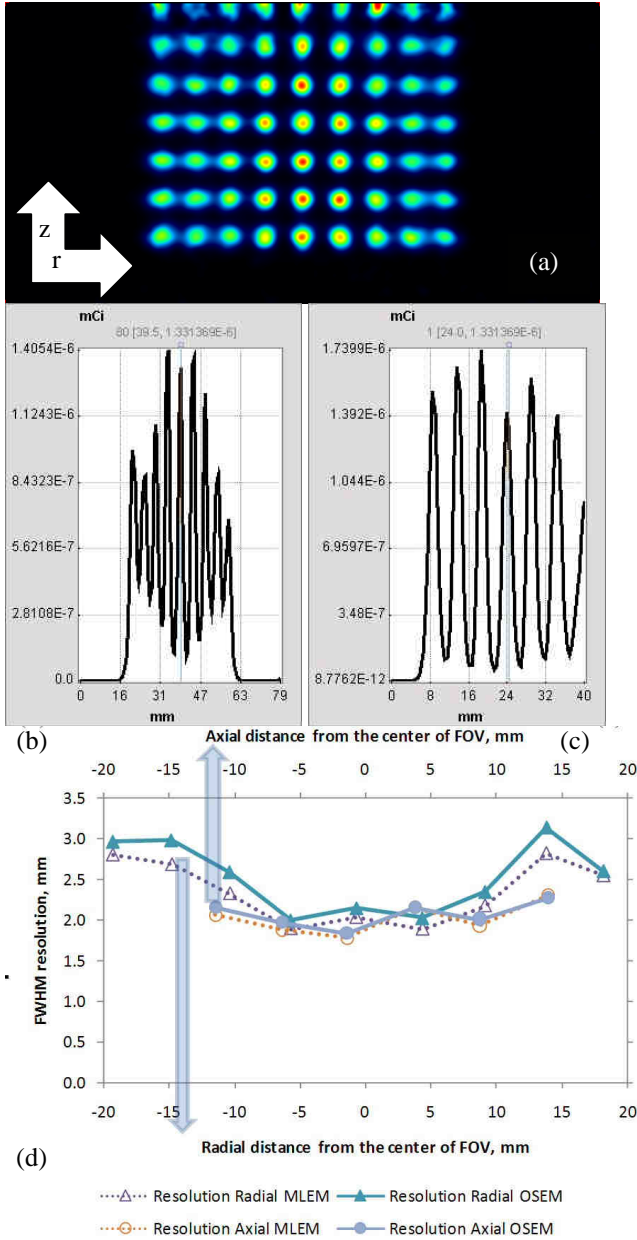


Fig. 5. ^{22}Na grid source OSEM reconstructed image in radial-axial plane (a), a line profile through the center of the FOV in radial direction (b), and axial direction of the scanner (c). (d) shows radial and axial FWHM spatial resolutions of the scanner calculated from the image in (a) employing the OSEM and MLEM algorithms.

III. SCANNER PERFORMANCE

We checked the spatial resolution with a grid of 9×9 ^{22}Na sources, each of 0.5 mm diameter at 5 mm spacing, all with the same activity level (555 kBq total), approximately centered in the FOV. The spatial resolution varies from 2 mm (FWHM) at the center of the FOV to 3 mm at 20 mm sideways from center of FOV. Fig. 5 shows the image in OSEM reconstruction (a), the activity profile in radial (b) and axial (c) directions and the Gaussian fitted FWHM resolutions in both directions (d).

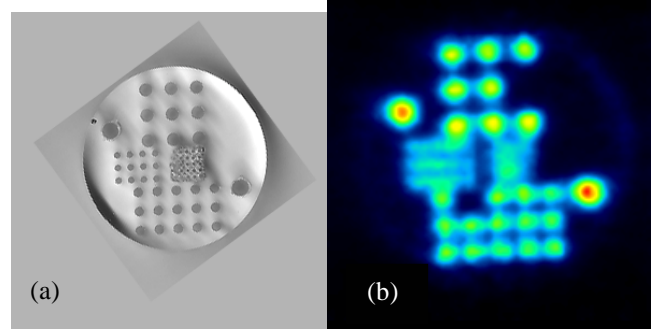


Fig. 6. (a) Derenzo type phantom photo: first row: one $\varnothing 2.5$ mm hole, 3×3 grid of $\varnothing 2$ mm holes separated by 4 mm; second row: 4×3 grid of $\varnothing 1$ mm holes separated by 2 mm; 5×5 grid of $\varnothing 0.5$ mm holes separated by 1 mm; third row: 5×3 grid of $\varnothing 1.5$ mm holes separated by 3 mm; one $\varnothing 2.5$ mm hole. (b) Image after 3 OSEM iterations from data acquired with the phantom in (a) filled with 18-FDG. The $\varnothing 1.5$ mm holes separated by 3 mm that are visible in the lower part in (a), can be clearly identified in the reconstructed image (b).

The resolution is slightly better with MLEM image reconstruction. We used 12 MLEM iterations and 3 OSEM iterations. De-convolving the 0.5 mm voxel size from the spatial resolution point spread function using square root error propagation improves the system's resolution it by 0.3 – 0.4 mm.

The resolution at the center of FOV was further checked with Derenzo-type phantom loaded with 18-FDG. In one can see that the $\varnothing 1.5$ mm, holes separated by 3 mm can be distinguished.

A. Mouse phantom

We use a physical mouse phantom to simulate the animal in the FOV. The phantom is a PTFE cylinder of $\varnothing 30 \times 70$ mm³ with a tubing of $\varnothing 1.05 \times 60$ mm³ filled with 100 μl of 18-FDG. To check the noise equivalent count (NEC) rate and saturation levels we loaded the phantom with 37 MBq of 18-FDG. The system was saturated down to 9.2 MBq. At this level the system count rate was 30k coincidences per second. The system is saturating mainly due to the signal sign inversion at the anode of the position sensitive photomultiplier at high rate. The time coincidence window used was 5 ns.

Below 9 MBq the system becomes proportional in recalculated concentration of activity vs. loaded concentration. NEC rate reached the maximum of 25.6 kcps at 7.4 MBq. The scatter level is about 9% and random counts are only about 4% at the activity corresponding to maximum of the NEC curve.

B. Syringe phantom

The mouse phantom produces a significant amount of counts coming from the area outside FOV, so to check the response in the center of FOV we prepared a 5 ml syringe loaded with 1 ml of 18-FDG located in the center of FOV.

For this type of phantom the saturation level is the same as for the mouse phantom. The maximum of NEC is at 7.4 MBq, reaching 25 kcps with 3% scatter level and 1% random counts.

IV. APPLICATION IN ISCHEMIA STUDY

High resolution PET scanners are ideally suited for translational research. We applied the Albira compact PET system for studying stroke-induced ischemia animal model. The ischemic penumbra is a major focus of the stroke research. In the ischemia study we tried to develop the model for delineation and evolution of penumbra [3] in temporal medial cerebral artery occlusion (tMCAO) and permanent medial cerebral artery occlusion (pMCAO). We used Fisher rats around P60. tMCAO and pMCAO was induced according to model proposed in [4]. tMCAO was maintained for 75 minutes. Two hours after the end of operation an MRI scan was performed, and then four hours after operation the first PET image was taken. The procedure for MRI and PET data acquisition was repeated at 24 h and 48 h after operation.

Fig. 7 shows the ischemic right cortex in an image taken 24 h after the operation. The outline in orange in Fig. 7(c) shows that while the part of the cortex of the MRI image in whiter color shows necrotic area (increased water content from dead cells), that neighboring area shows lower FDG uptake (penumbra).

V. CONCLUSION

The Albira small animal PET scanner is a flexible tool for brain and whole body imaging of small laboratory animals. The system has achieved a spatial resolution of 1.5 mm in the centre of the field-of-view, which is expected to further improve once the depth of interaction measurements that the system provides is incorporated in the image reconstruction schemes employed. At the same time, the exploitation of the DOI information is expected to provide a more uniform distribution of the spatial resolution as we move away from the centre of the FOV. The implemented fast image reconstruction and visualization tools, as well as the advanced image processing tools incorporated in the system make it a very useful tool in translational research and drug development.

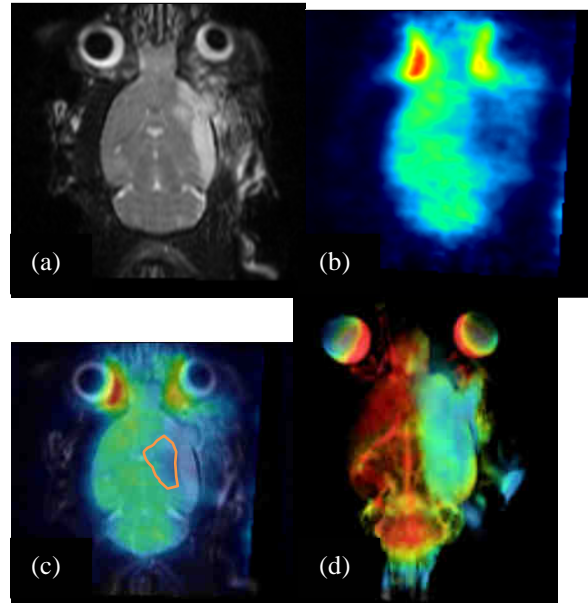


Fig. 7. Horizontal plane image of ischemic rat (pMCAO) area 24 hours after operation: (a) MRI T2 weighted in grayscale; (b) PET image with OSEM image reconstruction (red color corresponds to high activity concentration, blue color corresponds to low activity concentration, and black to no activity); (c) fusion of the images in (a) and (b) after co-registration with PMOD; (d) 3D rendering of the brain using PMOD - MRI texture volume rendered with PET texturing. The ischemic area in the animal's brain is shown in blue in the PET image (decreased FDG uptake) in the left cortex. The marked with orange is an area with lower FDG uptake, while this damage can not be perceived in the corresponding MRI image.

REFERENCES

- [1] PMOD Technologies Ltd; Sumatrastrasse 25; 8006 Zürich; Switzerland; tel. +41 (44) 350 22 37; <http://www.pmod.com>
- [2] S. Jan *et al.* "GATE: a simulation toolkit for PET and SPECT." *Phys. Med. Biol.* vol. 49, pp. 4543-4561, Oct. 2004
- [3] Astrup J, Siesjö BK, Symon L. "Thresholds in cerebral ischemia - the ischemic penumbra." *Stroke.* vol.12, pp. 723-5, Nov 1981
- [4] Hurtado *et al.* "Inhibition of glutamate release by delaying ATP fall accounts for neuroprotective effects of antioxidants in experimental stroke." *FASEB J.* vol. 17, pp. 2082-4, Nov 2003